Proceedings of 2004 Korea-Japan Joint Seminar
on Particle Image Velocimetry
POSTECH, Korea, Dec. 9 - 10

PIV measurement of oscillatory flow in a micro-channel as a bronchiole model

Won-je LEE *[1], Massaki KAWAHASHI *[2] and Hiroyuki HIRAHARA*[3]

*1 Graduate School of Science and Engineering, Saitama University, 255 Shimo-Okubo, Saitama-shi, Saitama 338-8570, Japan wonje@hanmail.net
*2 Department of Mechanical Engineering, Saitama University mkawa@mech.saitama-u.ac.jp
*3 Department of Mechanical Engineering, Saitama University hhira@mech.saitama-u.ac.jp

Abstract: The improvement of artificial respiration method has brought about the decrease in mortality of pulmonary diseases patients. Various respiratory curative methods, inclusive of HFOV (High Frequency Oscillatory Ventilation), have been developed for more effectual and less harmful management of acute respiratory failure. However, the mechanism of gas transfer and diffusion in a bronchiole has not yet been clarified in detail. As a first approach to the problem, we measured oscillatory flows in a Y-shaped micro-channels as bronchiole model by micro Particle Image Velocimetry(micro PIV). In order to establish the fundamental technique of PIV measurements on oscillatory air flow in a micro-channel, we used about 500-nm-diameter incense smoke particles, a diode laser, a high speed camera including an objective lens, and a HFOV, which is effective technique for medical care of pulmonary disease patients, especially, infants. The bronchiole model size is that parent tube is 500μm width and 500μm depth, and daughter tubes are 450μm width and 500μm depth. From this study made on the phenomenon of fluid in micro size bronchus branch of a lung, we succeeded to get time series velocity distribution in a micro scale bronchial mode. The experimental results of velocity distribution changing with time obtained by micro PIV can give fundamental knowledge on oscillatory airflow in micro-channel.

Keywords: Micro PIV, oscillatory flow, bronchial tube, human lungs, HFOV

1. Introduction

The main objective of this paper is to establish the investigation of oscillatory flow in a micro channel of bronchiole model by using micro PIV. Pulsatory or oscillatory gas flows in micro-channels are observed in certain engineering devices and biological structure. This is the fundamental fluctuation of flow in the arterial blood, reciprocating compressors, and respiratory organs. A typical case is the oscillatory airflow in bronchioles of the human lung. Over the past few years, several studies have been made on this phenomenon by way of experiment and a theoretical study.

Early measurements on secondary flow in a bifurcation model were achieved (et al., Schroter 1968). Sarangapani R. and Wexler A. (1999) have simulated the bifurcation model of aerosol bolus dispersion using fluid dynamics analysis package. Fresconi F.E. presented expiration flow in a symmetric bifurcation by using PIV and LIF. (et al., Fresconi F.E., 2003). And, Yamanadka et al.,(2003) determined the flow measurement on oscillating pipe flow near the entrance using the UVP method. Also, the advent of micro-electromechanical systems (MEMS) technology has made

possible the fabrication of complex fluid flow systems. In addition, micron-resolution particle image velocimentry(micro-PIV) has been developed to measure instantaneous and ensemble-averaged flow in micron-scale fluidic devices. Over the past few years, several studies have been made on micro-PIV, for instance, Hele-shaw flow (e.g., Santiago, 1998), silicon micro channel flow (e.g., Meinhart, C., 1999), blood cell, inkjet printer device (e.g., Meinhart, C. D, 2000), electro-osmosis-driven micro-channel (e.g., Kim, 2002). However, micro-PIV studies, for the most part, have focused on the liquid environment. While fluorescently labeled particles are well suited for micro-PIV studies in liquid flows, the methods are not readily applicable to high-speed airflows for several reasons. For example, the flow of seeding gas remains a significant problem in micro-PIV. To overcome this situation, we carried out the flow visualization and velocity measurement with micro PIV in the micro-channel as bronchiole model. Since an oscillatory flow in bronchiole duct is very complex, micro PIV is most suitable to obtain an instantaneous velocity field.

In this paper, first basic theory of human lungs, the variety of mechanical ventilation, the definition of HFOV, experimental setup has been described. And we presented the experimental conditions, initial HFOV settings, and the results obtained by micro PIV. Finally, we summarized some conclusions including a future study works.

2. Experimental Setup and Method

2.1 Human lung background

The respiratory airflow begins in the mouth and nose. Air enters and exits the lungs through trachea, bronchi, and alveoli. The air moves back out again by way of the same airway passages. The alveoli are surrounded by capillaries of the blood system. The actual respiratory surfaces are the walls of the numerous alveoli in the lungs.

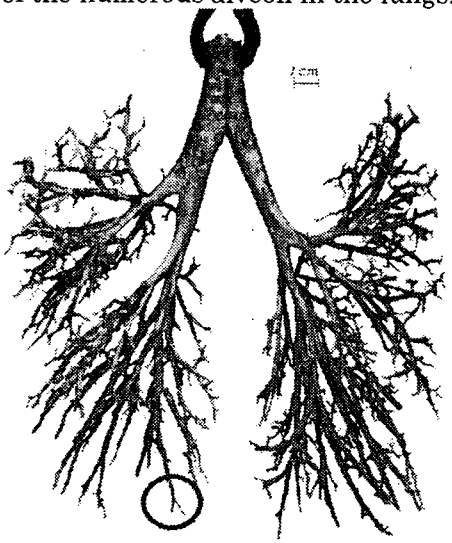

Fig. 1. The bronchial tree

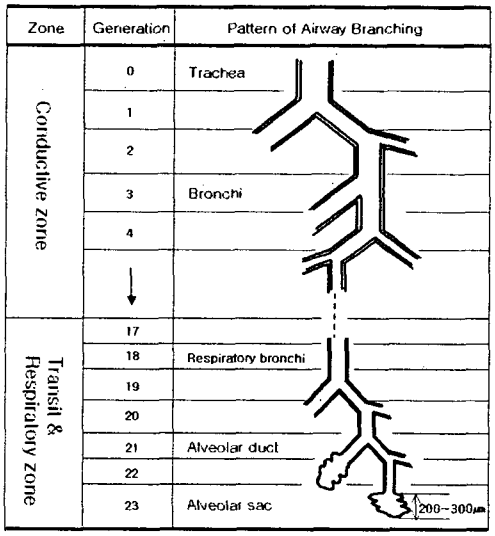

Fig. 2. Pattern of Airway Branching

Fig. 1 shows the bronchial tree in a lung inside. As the Fig. 1 indicates, lung is very complex structure. Weibel (1963) provided the quantitative measurements of the lung's length, diameter. Fig. 2 summarizes the composition of the airways. To quote Weibel (E. R. Weibel, 1963), Generations 0~16 are the conduction airways, and generation 17~23 compose the respiratory airways. As the pattern of airway branching, Lung has about 23 branches. The structures of lung is complicated by compliant walls and a thin lining of mucus. The main breathing is divided according to region. One is trachea, bronchus. The other is alveolus with gas exchange. Lung structure is composed of the trachea, branch off two large tubes. These tubes are called the main stem bronchi. The tiniest tubes are called bronchioles, and there are about 30,000 of them in each lung. At the end of each bronchiole is a special area that leads into clumps of tiny air sacs called alveoli. There are about 600 million alveoli in our lungs. Each alveolus has a mesh-like covering of very small blood vessels called capillaries. The alveoli are tiny hollow sacs 200-300 microns in

diameter.

At normal conditions of respiration, the tidal ventilation volume of adult is about 500 *ml* . The inhaled air fills the trachea, the bronchi and the bronchial, and it contacts with the physiologically residual air at the respiratory bronchiole and the alveolar ducts. The inhaled air does not reach directly to the alveoli, and the gas exchange occurs at the region of the respiratory bronchiole and the alveolar duct. The part of the air filled from the trachea to the respiratory bronchiole does not be involved in the gas exchange, and it is called the dead space ventilation volume. It is about 150 *ml* . The end part of lung at which the inhaled air contacts with the residual air, has complicated bronchiole tissue with bifurcated micro-channels in which the complicated gas exchange mechanism must be occurred by not only molecular diffusion but also fluid motion. The fundamental parameters for this oscillatory flow are Reynolds number(Re) and Womersley number(W). At the end part of lung, Re number is very low, and in the case of normal respiration, W number is also very small because the frequency of respiration is very low (about 0.2 Hz). It means that the oscillatory flow in the bronchiole can be assumed as quasi-steady laminar flow. When HFOV is applied as artificial ventilation, the characteristics of oscillatory flow in bronchiole change markedly by the mode of HFOV. In the typical mode of HFOV, the tidal volume is less than it in the natural respiration, and the frequency is in the range of about 5~20Hz. The frequency ratio is about 25~100 by comparison with the normal respiration frequency. The increase of the frequency ratio brings about the increase of W number. It means that there is possibility of appearing unsteadiness of oscillatory flow in bronchiole, and it causes the generation of the different mechanism of the gas exchange in the lung system. Moreover the flow pattern in the trachea and the bronchi is certainty different from the flow pattern in the alveolar duct and the alveoli. Reynolds number (*Re*) is from about 4350 at the trachea to 34 at the terminal bronchus. And the *Re* number in the alveolar region is less than 0.04. These alveoli inflate with inhalation and deflate with exhalation. The Reynolds number is different each region in human lungs airway. Especially, The Re number in the alveolar region is less than 0.01, depending on breathing conditions. Hence the average fluid velocity at the center of the alveolar sac will be zero. Therefore, the flow field in the alveoli seems to be a streaming velocity and the fluid velocity at the alveolar sac is assumed to be the streaming velocity. In order to clarify the gas exchange mechanism both in the case of the normal respiration and HFOV, the detailed analysis of flow in lung system is required. However, direct measurement of oscillatory airflow through the real lung is very difficult, especially in the end part of the lung.

2.2 Mechanical ventilation

Over the past 40 years, mechanical ventilation has been conducted for the improvement of health in treatment of various forms of respiratory failure. The goal of the mechanical ventilation manipulates alveolar ventilation. It improves oxygenation and lung volume. And it reduces work of breathing. The classification of ventilation divides widely into two classes of positive pressure ventilation and negative pressure ventilation. There are variety of ventilation such as CMV (Control Mode Ventilation), AMV (Assist Mode Ventilation), IMV (Intermittent Mandatory Ventilation), CPAP (Continuous Positive Airway Pressure), PSV (Pressure Support Ventilation), and HFOV (High Frequency Oscillation Ventilation). In the mechanical ventilation, pressure target (pressure control) ventilation has an initially rapid flow. An advantage of this method has a rapid assist for critical care. A disadvantage cannot be applied guaranteed volume during spontaneous breathing.

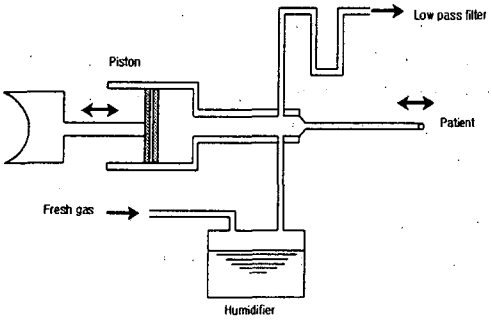

Fig. 3. Foundation circuit of HFOV

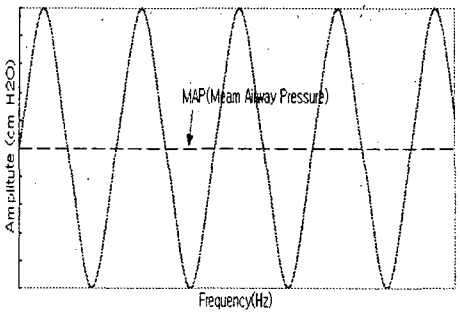

Fig. 4. Mode of HFOV

Fig. 3 shows the foundation circuit of HFOV (Humming II) manufactured by *Metran Co.,Ltd.* Component of HFOV consists of a humidifier and a pump, including piston. Fig. 4 shows the mode of HFOV. During a reciprocating motion of piston in pump, HFOV produces a harmonic wave of ratio I/E=1:1. (Here, I/E=Inhalation/Exhalation). The main determinant of oxygenation and ventilation is the MAP (Mean Airway Pressure), the amplitude of stroke, and the frequency. In this study, we used to this HFOV instrument and applied the experimental data of frequency, amplitude, MAP, pressure (Pa) of inlet zone of micro channel as shown table 3.

2.2 Experimental setup

The experimental setup of micro-PIV system is shown in Fig. 5. As the flow moves deeper the lungs, the flow pattern becomes more complex with the more complicated merging of flow from varies daughter branches. The geometry of the bronchiole model for this study was chosen as typical from the region marked by the red circle (See Fig.1, Fig.6). This region is one of part in generation 18-20 from mouth (trachea). The measurement section of a Y-junction was a rectangle micro-channel made of steel plate with parent tube of 500μm width, 500μm depth, 200mm length, and daughter tubes of 450μm width, 500μm depth, and 200mm length. The branching angle between the parent and daughter tube was 60°, regular of most bifurcations in the airway branching. The rounding between daughter tubes was R5. Its details are shown in Fig. 6. The oscillatory motion is forced by HFOV (Humming II) manufactured by *Metran Co.,Ltd.* Frequency and amplitude of HFOV can be changed on the front panel controls. An oscillating piston placed in the HFOV apparatus was driven by electrical motor. The HFOV was connected to micro-channel though a tube. The illumination beam produced by diode laser (IR-4, IDT), which wavelength is 800 nm, power is 4W. This laser generates high-energy infrared radiation that can pose serious risks to eye safety. Infrared radiation is invisible to the eye, so the hazard is not immediately obvious, but the radiation can be focused onto the retina. Laser beams are also intense enough to burn skin, clothing or paint. For the same reason the rays of the laser beam should not hit the CCD camera sensor directly. Therefore, the laser beam was collimated to illuminate the test section of the back of the Y-junction at an angle of 60 degrees. Images were captured using a high-speed camera (X-Stream™ XS-4) which resolution is 512(H)×512(V) pixels in space and 10 bits depth in intensity. An objective lens (KEYENCE VQ-Z50A, High magnifying power 500) was used for magnification of the images. Fig. 7 is a raw image. This image was captured using a high-speed camera. The raw image was useful to calculate a velocity vector field. In order to calculate, we analyzed using algorithm of conventional cross-correlation method (Interrogation resolution 32 × 32 pixels). However, the raw image contains a high percentage of reflection at the apex surface. The effect of reflection occurs trouble things such as error vectors. It remains an unsolved problem. Moreover other PIV researchers become an issue yet. In order to achieve the gas flow field in this study, we used the seeding gas particles (approximately 500-nm-diameter) produced by burning as shown Fig.5. The temperature of the test fluid was maintained at 20°C(standard room temperature) as shown in table 1.

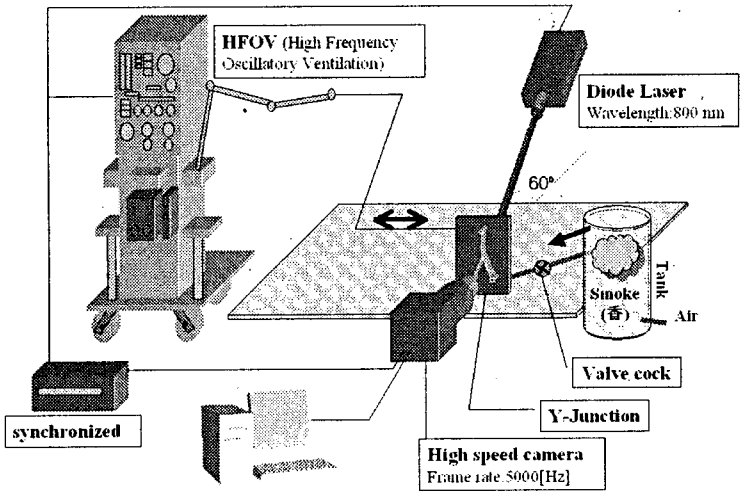

Fig. 5 Experimental set-up of micro-PIV system

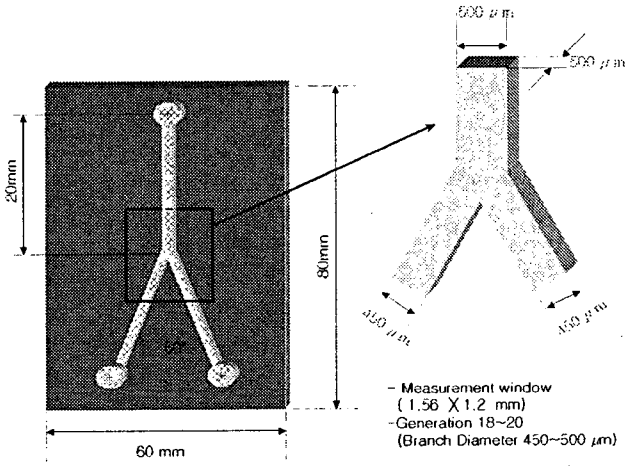

Fig. 6 Schematics of Y-junction of a micro-channel

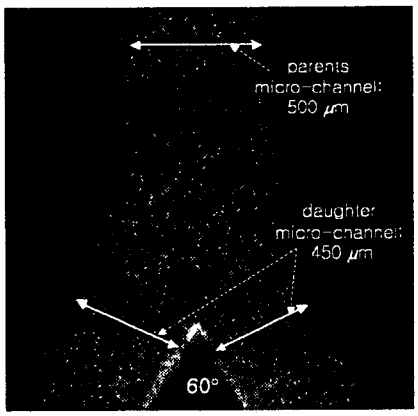

Fig. 7 raw image

Table 1. Experimental parameters

Parameters	Value
Model	
- Parents tube scale [μm]	500W × 500D
- Daughter tube scale [μm]	450W × 500D
Diode laser (IR-4, IDT)	
- Wavelength	800 nm
- Power	4 W
High speed camera (X-Stream™ XS-4)	
- Image recording [pixels]	512H × 512V
- Recording frames	1,000
- Frame rate [Hz]	5,000
- Time between two frames [μs]	200
PIV interrogation algorithm	Cross-correlation
- Interrogation resolution	32 × 32 pixels
Measurement window size	1.5 × 1.5 mm
Seeding particle	Incense smoke (diameter 500nm)
The temperature of the test fluid	20°C(standard room temp.)

3. Results and discussion

3.1 Velocity distributions

In order to show the flow phenomenon in lungs, the measurements of oscillatory flow in a model of bronchial tubes were made by a Micro PIV. Instantaneous velocity vector field results were obtained at influx and efflux under HFOV of oscillatory airflow. This velocity fields were measured using a high-speed camera (1000 frames/0.2sec), a diode laser, and micro-PIV system. It was calculated based on of instantaneous micro PIV measurement results.

To examine the experimental investigation in the micro-channel as bronchiole model, I had to clarify dimensionless factor first. Dimensionless parameters covered in this study is $\mathrm{Re}_\delta = 2.659$, $W = 0.626$, which are the frequency 15Hz in this experiments.

The stokes layer thickness, δ , is given by

$$\delta = \sqrt{\frac{2\nu}{\omega}} \tag{1}$$

here, ν is kinematics viscosity[$\nu = 1.513\times10^{-5}$ m^2/s, 20°C, air] and ω is angular frequency[$\omega = 2\pi f$].

The acoustic Reynolds number, Re_δ is calculated by

$$\mathrm{Re}_\delta = \frac{2u'}{\sqrt{\nu\omega}} \tag{2}$$

here, u' is the piston velocity amplitude as $u = u' \cos\omega t$.

Shear Wave Number (Womersley Number), w is calculated by

$$w = \frac{D}{2}\sqrt{\frac{\omega}{\nu}} \tag{3}$$

here, D is the diameter of the micro channel. The dimensionless parameters used in this study are shown in Table 2.

Table 2. Dimensionless parameters in this experimental case

Experimental	Value
Stokes layer thickness, δ[mm]	0.564
Reynolds number, Re_δ	2.12
Shear Wave number (Womersley number), W	0.627
Flow pattern	Quasi-steady laminar

As has already been mentioned in sect. 2.1, at the micro-channel, Re number (eq.2) and W number (eq.3) were very small. It means that this flow is quasi-steady laminar flow for slow oscillations. The velocity distribution has the same phase as the pressure gradient. However, the Stokes layer thickness, δ[mm] (eq.1) was lager than diameter [0.5mm] of micro channel in this study. It means that oscillatory flow in this micro-channel also is assumed quasi-steady laminar flow even if high frequency.

Table 3 shows the experimental condition of HFOV and flow rate and pressure of inlet zone of micro channel in this measurement. The volume of MAP was fixed on 4cmH_2O with the main determinant of oxygenation in HFOV. On the other hand, the range of frequency and amplitude of stroke was chosen 15Hz and 14 cmH_2O with the main determinant of ventilation in HFOV. Flow rate and pressure of outlet zone from HFOV were 1.346 *ml* /sec, 1360 Pascal. This data was calculated in relation to stroke volume [30 *ml* /1V] and pressure[10 mV/1cmH_2O] as shown table 3, Fig 8. And bypass apparatus introduced between the outlet of HFOV and inlet of micro-channel in order to control high flow rate and pressure. Flow rate and pressure of inlet zone of micro channel was each 0.02 *ml* /min, 370 Pascal. Fig.8 shows the timing diagram of different stroke volume and pressure by using oscilloscope. This diagram illustrates the variation of the stoke volume and

pressure with time.

Table 3 Experimental condition of HFOV

Condition	Value
Frequency (Hz)	15
Amplitude (cmH_2O)	14
MAP (Mean Airway Pressure, cmH_2O)	4
Stroke volume	30 *ml* / 1V
Pressure	10 mV / 1cmH_2O
Flow rate of HFOV (*ml* /sec)	1.346
Pressure of HFOV (Pa)	1360
Flow rate of inlet zone of micro channel (*ml* /sec)	0.02
Pressure of inlet zone of micro channel (Pa)	370

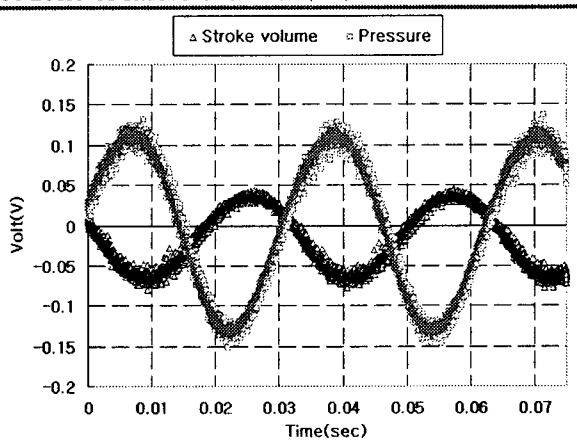

Fig.8 Timing diagram of different stroke volume and pressure in HFOV

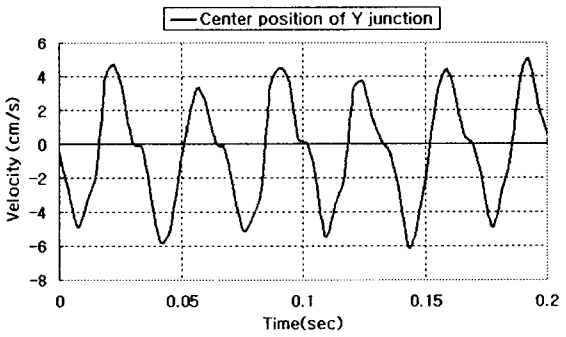

Fig.9 Velocity profiles of spatial center position at the Y junction of micro-channel.

Figure 9 shows the velocity profiles for spatial center position of the Y micro-channel. This profile shows the entire positive or negative velocity at different times within 6 periods. As the diagram indicates, the instantaneous velocity profile has a fluctuation caused by the uncertainty of the measurement.

Figure 10 (a)-(d) shows the velocity profile of the oscillatory flow at different and the stream-wise velocity profiles in the Y shaped micro-channel at A-A, B-B sections times during on cycle of oscillation. In Fig. 10(a) during influx the peak velocity occurs near the centerline of axial direction at $\phi=3\pi/4$. The velocity profile in the daughter branches was a slanting flow motion from the parent branch. In Fig. 10(b), at $\phi= 5\pi/4$, during efflux the flow fluid from the both daughter branches merges in a junction of the parent tube. The velocity of centerline decreases for a little while due to merge. However the axial flow pattern is quickly transformed into a velocity peak. This transformation is caused by the secondary flows arises in the parent tube. Fig. 10(c), (d) shows point-wise comparison of the cross-stream velocity at A-A, B-B sections in order to understand

velocity distribution of local information. The cross-stream velocity distribution, at A-A section, shows that the peak velocity is also larger than near the wall surface during an influx in Fig 10(c). And the velocity distribution of the influx changes during each phase. It can be seen from these figures that velocity distribution is almost zero, for 0 and 2π. And the velocity distribution is gradually increases and decreases during the different phase, continuously. The velocity distribution is moved into the lower part during times $\phi=0$, $\pi/4$, $\pi/2$, $3\pi/4$, and π, which corresponds to the negative velocity. At times $\phi=5\pi/4$, $3\pi/2$, $7\pi/4$,and 2 π, velocity distribution shows reversal flow. As has already been mentioned above, even though the frequency was high (15hz), this oscillatory flow was quasi-steady laminar flow in the micro-channel as shown in Fig.10(c). The velocity distribution has the same phase as the pressure gradient. Fig 10 (d), at B-B section, shows also the velocity distribution is gradually s increase and decrease during the different phase.

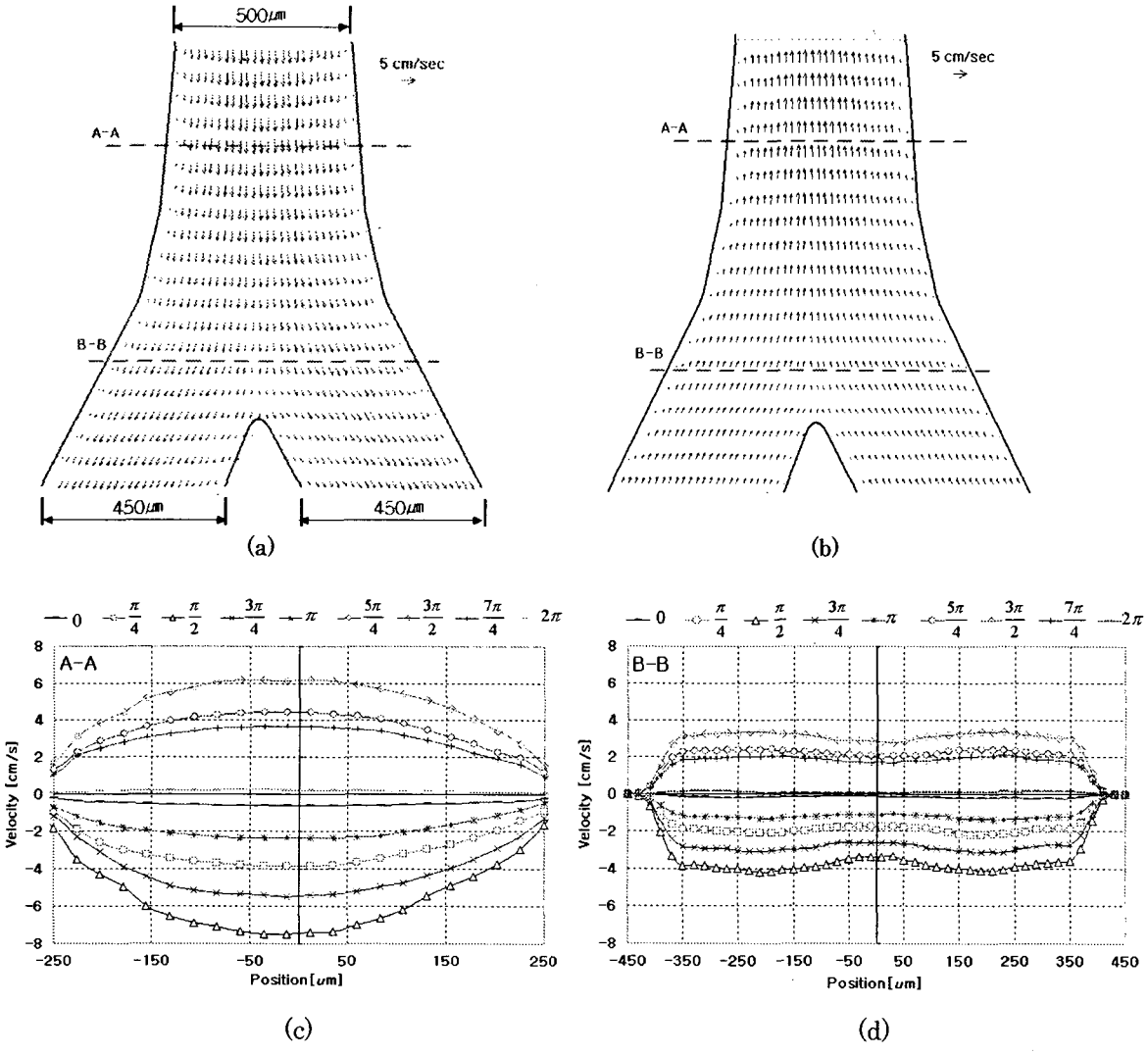

Fig. 10 Velocity vector fields and the stream-wise velocity profiles in the Y shaped micro-channel at A-A and B-B sections. The velocity fields are measured using a high-speed camera, a diode laser, and micro-PIV system under HFOV drive. (a) Velocity filed at the influx, $\phi=3\pi/4$. (b) Velocity filed at the efflux, $\phi=5\pi/4$. (c) Instantaneous velocity profiles for one period at A-A section. (d) Instantaneous velocity profiles for one period at B-B section.

Figure 11(a)-(d) shows path line of the particles motion in the Y micro-channel. The path lines are shown at one cycle. Fig. 11(a) Particles positions [1-7] from initial time t=0ms ($\phi=0$). Fig. 11 (b), (c) particles positions at time delay Δt =8.2, 16.4 ms ($\phi=\pi/2$, π). Fig. 11 (d), (e) particles position at time delay Δt =24.6, 32.8ms, ($\phi=3\pi/2$, 2π) shows reversal flow during an efflux.

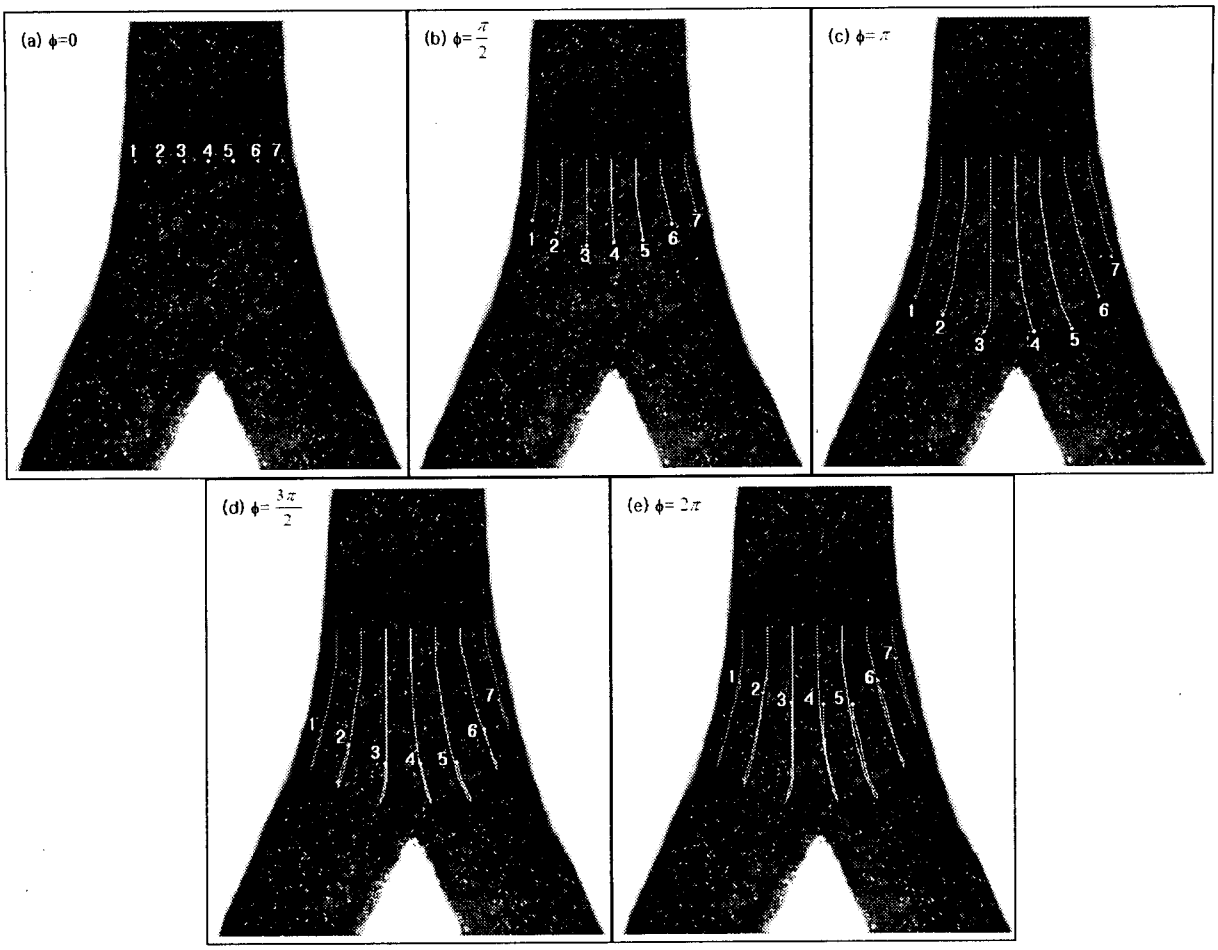

Fig.11 Path line shows the particles motion of the Y micro-channel.

6. Conclusion

From these results, we make next conclusions. For visualization of bronchial tube, first the experimental object made of Y shaped micro channel of a symmetric bifurcation that parent tube(500 μm wide,500 μm deep) and daughter tubes(450 μm wide,500 μm deep).

The oscillatory flow in bronchial were observed by Micro PIV technique under the HFOV. We acquired the good agreement on study of process of oxygenation and ventilation in the microscopic bronchial tube. During influx the peak velocity occurs near the centerline of axial direction. The velocity profile in the daughter branches was a slanting flow motion from the parent branch. During efflux the flow fluid from the both daughter branches merges in a junction of the parent tube. The velocity distribution of the influx changes during each phase. It can be seen from these figures that velocity distribution is almost zero, for 0 and 2π. And the velocity distribution is gradually increases and decreases during the different phase, continuously. The velocity distribution is moved into the lower part during times ϕ=0, π/4, π/2, 3π/4, and π, which corresponds to the negative velocity. At times ϕ=5π/4, 3π/2, 7π/4,and 2 π, velocity distribution shows reversal flow. Form these velocity distributions the oscillatory flow in the micro channel as bronchiole model confirmed as quasi-steady laminar flow.

Through this work, we know oscillatory flow pattern and effects with the bronchial tube of single bifurcation and these results expected to help in-coming work for design or medical treatment techniques of mechanical ventilation. Also, this analysis may be helpful to consider some important factors of achieving a successful treatment of pulmonary disease.

Actually, the volume of lungs changes every time. When we breathe in, air fills the lungs and the lungs get bigger. When we breathe out, air comes out and the lungs get smaller. The lungs

inflate with inhalation and deflate with exhalation. To observe the truly flow of flexible lungs, a future computational simulation of using a fluid dynamics analysis package is needed.

In order to obtain the gas exchange mechanism both in the case of the normal respiration and HFOV, the detailed analysis of flow in lung system is required. Also both experiment of each parameter (volume, pressure, flow rate, frequency) and interrelationship with each other must be examined carefully.

References

Fresconi F.E., Wexler A.S., Prasad A.K., 2003, "Expiration flow in a symmetric bifurcation", Exp. in Fluids, 35, 493-501

Meinhart C. D., Hongsheng Zhang, 2000, "The Flow Structure Inside a Micro fabricated Inkjet Printhead", J. of microelectromechanical systems, vol.9, No.1, 67-74

Meinhart C. D., Wereley S. T. and Santiago, J. G., 1999, "PIV Measurement of a Micro channel Flow", Exp. in Fluids, 27, 414-419

Robert A., Freitas Jr., 1999, "Nano medicine", Volume I: Basic Capabilities, Landes Bioscience, Georgetown, TX

Santiage J. G, Wereley S.T., Meinhart C.D., Beebe D.J., Adrian R.J., 1998, "A particle image velocimetry system for micro fluidics", Exp. in Fluids 25, 316-319

Sarngapani R. and Wexler A. S., 1999, "Modeling aerosol bolus dispersion in human airways", J. Aerosol Sci. Vol. 30. No. 10 pp. 1345-1362

Schroter R. C. and Sudlow, M. F., 1969, " Flow patterns in models of the human bronchial airways", Resp. physiol.7,341

Weibel E.R., 1963, "Morphometry of the human lung", Academic Press, New York